Electronic Supplementary Material (ESI) for Physical Chemistry Chemical Physics.
This journal is © the Owner Societies 2021

Supplementary Information for: Efficient and low-scaling linear-response time-dependent density functional theory implementation for core-level spectroscopy of large and periodic systems

Augustin Bussy & Jürg Hutter

Department of Chemistry, University of Zurich, Winterthurerstrasse 190, CH-8057 Zürich, Switzerland.

augustin.bussy@chem.uzh.ch, hutter@chem.uzh.ch

1 Basis convergence studies

We give here the K-edge basis convergence results. The energy difference between the first and second (ω_2-ω_1) excitation energies are reported across the pcseg and pcX basis sets using different standard hybrid functionals. The EOM-CCSD values comes from Ref. 1 and the experimental values from Refs. 2, 3, 4 and 5. The H_2O oxygen K-edge convergence test is displayed on figure 1, NH_3 nitrogen K-edge on figure 2, the CO carbon and oxygen K-edge on figures 3 and 4 and the C_2H_4 carbon K-edge on figure 5. Note that on all figures, basis sets range from doule zeta quality (pcseg-1, pcX-1) to quintuple zeta quality (pcseg-4, pcX-4). Wide clear bars correspond to the pcseg basis and thin dark bars to pcX.

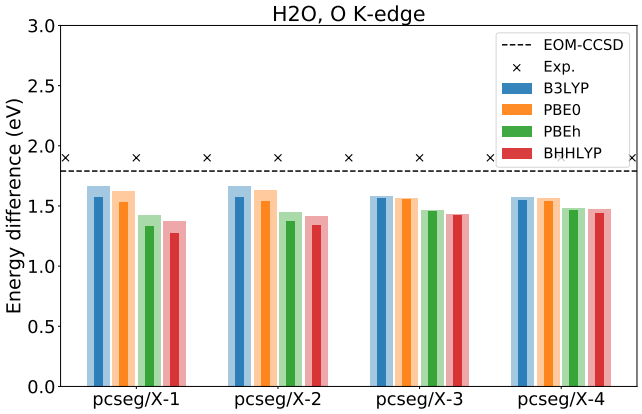

Figure 1 $\omega_2 - \omega_1$ at the oxygen K-edge of water for different functionals over basis sets of increasing quality.

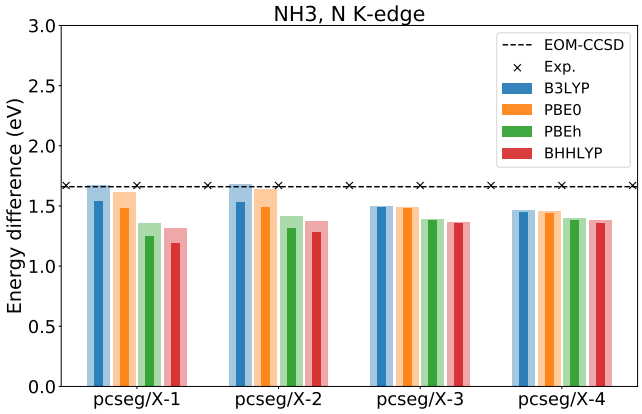

Figure 2 $\omega_2 - \omega_1$ at the nitrogen K-edge of amonia for different functionals over basis sets of increasing quality.

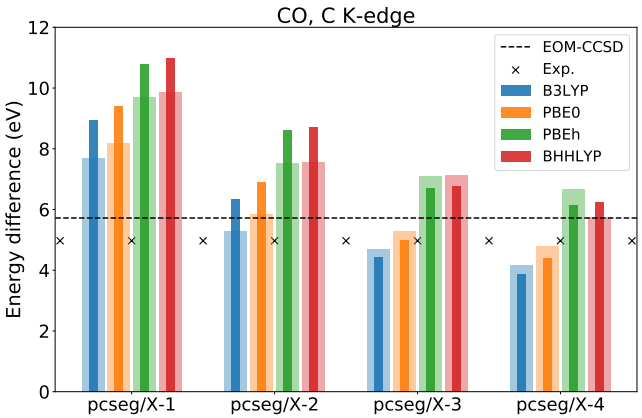

Figure 3 $\omega_2 - \omega_1$ at the carbon K-edge of carbon monoxide for different functionals over basis sets of increasing quality.

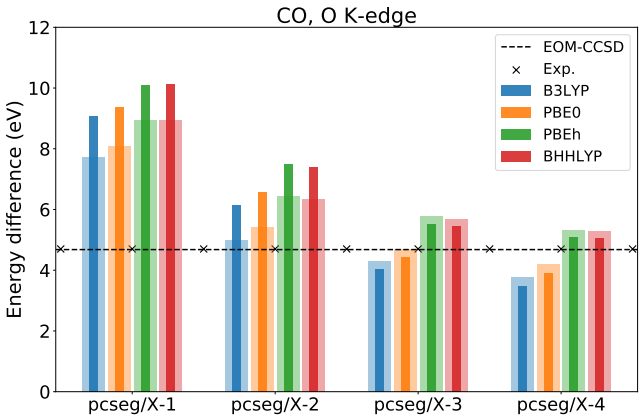

Figure 4 $\omega_2 - \omega_1$ at the oxygen K-edge of carbon monoxide for different functionals over basis sets of increasing quality.

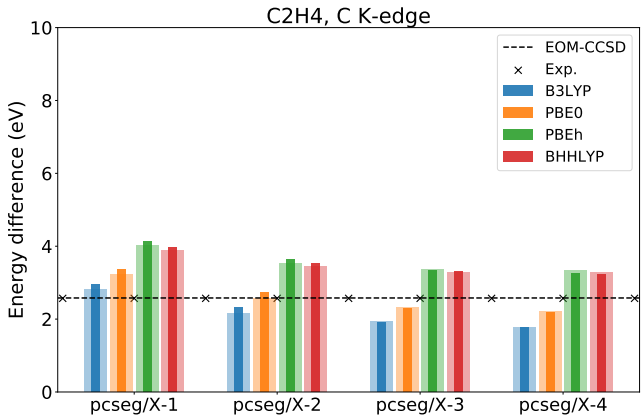

Figure 5 $\omega_2 - \omega_1$ at the carbon K-edge of ethene for different functionals over basis sets of increasing quality.

2 Detailed SOC matrix elements

We give here the detailed spin–orbit coupling matrix elements in the auxiliary many electron wave functions[6] (AMEW) basis. To keep the equations concise, we work within the Tamm-Dancoff approximation and restricted closed-shell systems (extensions to full TDDFT and/or open-shell systems are straight forward).

We assume that the ground state densities and KS orbitals are the same for both spins, *i.e.* $n^0_\alpha(\mathbf{r}) = n^0_\beta(\mathbf{r})$ and $\phi^0_{j\alpha}(\mathbf{r}) = \phi^0_{j\beta}(\mathbf{r})$. Then two types of excitation can take place, singlet excitation, where $n^-_\alpha(\mathbf{r}) = n^-_\beta(\mathbf{r})$ ($c^-_{pi\alpha} = c^-_{pi\beta}$), and triplet excitation, where $n^-_\alpha(\mathbf{r}) = -n^-_\beta(\mathbf{r})$ ($c^-_{pi\alpha} = -c^-_{pi\beta}$)[7]. These conditions can be imposed by construction when taking linear combinations of the linear response orbitals, such that:

$$u^-_{pi} = \frac{1}{\sqrt{2}}\left(c^-_{pi\alpha} + c^-_{pi\beta}\right) \tag{1}$$

describes singlet excitations and

$$v^-_{pi} = \frac{1}{\sqrt{2}}\left(c^-_{pi\alpha} - c^-_{pi\beta}\right) \tag{2}$$

describes triplet excitations. This leads to two different eigenvalue problems, one for each type of excitation. From the solutions u^-_{pi} and v^-_{pi}, we define the singlet and triplet LR orbitals, respectively:

$$\phi^s_{j\alpha}(\mathbf{r}) = \phi^s_{j\beta}(\mathbf{r}) = \sum_p c^{-,s}_{pi\alpha}\ \varphi_p(\mathbf{r}) = \frac{1}{\sqrt{2}}\sum_p u^-_{pi}\ \varphi_p(\mathbf{r}) \tag{3}$$

$$\phi^t_{j\alpha}(\mathbf{r}) = -\phi^t_{j\beta}(\mathbf{r}) = \sum_p c^{-,t}_{pi\alpha}\ \varphi_p(\mathbf{r}) = \frac{1}{\sqrt{2}}\sum_p v^-_{pi}\ \varphi_p(\mathbf{r}) \tag{4}$$

The corresponding AMEW expansions for singlet and (spin-conserving) triplets can then be written as:

$$|\Psi_S\rangle = \frac{1}{\sqrt{2}}\sum_i \left[\left(\hat{r}^s_{i\alpha}\right)^\dagger \hat{a}_{i\alpha} + \left(\hat{r}^s_{i\beta}\right)^\dagger \hat{a}_{i\beta}\right]|\Psi_0\rangle \tag{5}$$

$$|\Psi^0_T\rangle = \frac{1}{\sqrt{2}}\sum_i \left[\left(\hat{r}^t_{i\alpha}\right)^\dagger \hat{a}_{i\alpha} - \left(\hat{r}^t_{i\beta}\right)^\dagger \hat{a}_{i\beta}\right]|\Psi_0\rangle \tag{6}$$

where $|\Psi_0\rangle$ is the Slater determinant of the ground state orbitals, $\hat{a}_{i\sigma}$ is the annihilation operator for a ground state KS orbital i with spin σ and $\hat{r}^{t,s}_{i\sigma}$ the creation operator for the corresponding singlet/triplet LR orbital. Explicitly , if we write the ground state SD as:

$$|\Psi_0\rangle = |\phi^0_{1\alpha}\phi^0_{1\beta}\ \ldots\ \phi^0_{i\alpha}\phi^0_{i\beta}\ \ldots\ \phi^0_{N\alpha}\phi^0_{N\beta}\rangle, \tag{7}$$

the combined effect of $\left(\hat{r}^{s,t}_{i\alpha}\right)^\dagger \hat{a}_{i\alpha}$ on it is:

$$\left(\hat{r}^{s,t}_{i\alpha}\right)^{\dagger}\hat{a}_{i\alpha}|\Psi_0\rangle = |\phi^0_{1\alpha}\phi^0_{1\beta}\ \ldots\ \phi^{s,t}_{i\alpha}\phi^0_{i\beta}\ \ldots\ \phi^0_{N\alpha}\phi^0_{N\beta}\rangle \tag{8}$$

The spin-flip triplets (with spin quantum numbers $S = 1$ and $m_s = \pm 1$) are expressed as:

$$|\Psi^{+1}_T\rangle = \sum_i \left(\hat{r}^t_{i\alpha}\right)^{\dagger}\hat{a}_{i\beta}|\Psi_0\rangle \tag{9}$$

and

$$|\Psi^{-1}_T\rangle = \sum_i \left(\hat{r}^t_{i\beta}\right)^{\dagger}\hat{a}_{i\alpha}|\Psi_0\rangle \tag{10}$$

Given a one electron spin–orbit Hamiltionian H_{SO}, matrix elements of the type $\langle\Psi_S|H_{SO}|\Psi^0_T\rangle$ need to be evaluated. Because triplet and singlet LR orbitals are not necessarily orthogonal to each other, we cannot simply apply the Slater rule for evaluating matrix elements. Instead, we have to use Löwdin's rule[8]. Note that within XAS LR-TDDFT, the sum over orbitals i in equations (5), (6), (9) and (10) is restricted to the core excited states, which amount to 3 in case of $L_{2,3}$-edge spectroscopy. We label those core states with capital letters I, J to distinguish them. All non-zero necessary SOC matrix elements are given below.

SOC matrix elements between the ground state SD and excited triplets with secondary quantum number $m_s = -1, 0, 1$:

$$\langle\Psi_0|H_{SO}|\Psi^0_T\rangle = \frac{1}{\sqrt{2}}\sum_I\left(\langle\phi^0_{I\alpha}|H_{SO}|\phi^t_{I\alpha}\rangle - \langle\phi^0_{I\beta}|H_{SO}|\phi^t_{I\beta}\rangle\right) \tag{11}$$

$$\langle\Psi_0|H_{SO}|\Psi^{+1}_T\rangle = \sum_I\langle\phi^0_{I\beta}|H_{SO}|\phi^t_{I\alpha}\rangle \tag{12}$$

$$\langle\Psi_0|H_{SO}|\Psi^{-1}_T\rangle = \sum_I\langle\phi^0_{I\alpha}|H_{SO}|\phi^t_{I\beta}\rangle \tag{13}$$

SOC matrix element between excited singlets and excited triplets with secondary quantum number $m_s = -1, 0, 1$:

$$\begin{aligned}\langle\Psi_s|H_{SO}|\Psi^0_T\rangle = \ & \frac{1}{2}\sum_I\left(\langle\phi^s_{I\alpha}|H_{SO}|\phi^t_{I\alpha}\rangle + \langle\phi^s_{I\alpha}|\phi^t_{I\alpha}\rangle\left[\langle\phi^0_{I\beta}|H_{SO}|\phi^0_{I\beta}\rangle + \sum_i\sum_\sigma\langle\phi^0_{i\sigma}|H_{SO}|\phi^0_{i\sigma}\rangle\right]\right)\\ & -\frac{1}{2}\sum_I\left(\langle\phi^s_{I\beta}|H_{SO}|\phi^t_{I\beta}\rangle + \langle\phi^s_{I\beta}|\phi^t_{I\beta}\rangle\left[\langle\phi^0_{I\alpha}|H_{SO}|\phi^0_{I\alpha}\rangle + \sum_i\sum_\sigma\langle\phi^0_{i\sigma}|H_{SO}|\phi^0_{i\sigma}\rangle\right]\right)\\ & -\frac{1}{2}\sum_{I,J}\langle\phi^0_{J\alpha}|H_{SO}|\phi^0_{I\alpha}\rangle\langle\phi^s_{I\alpha}|\phi^t_{J\alpha}\rangle\\ & +\frac{1}{2}\sum_{I,J}\langle\phi^0_{J\beta}|H_{SO}|\phi^0_{I\beta}\rangle\langle\phi^s_{I\beta}|\phi^t_{J\beta}\rangle\end{aligned} \tag{14}$$

$$\begin{aligned}\langle\Psi_S|H_{SO}|\Psi^{+1}_T\rangle = & \frac{1}{\sqrt{2}}\sum_I\langle\phi^s_{I\beta}|H_{SO}|\phi^t_{I\alpha}\rangle\\ & -\frac{1}{\sqrt{2}}\sum_{I,J}\langle\phi^0_{J\beta}|H_{SO}|\phi^0_{I\alpha}\rangle\langle\phi^s_{I\alpha}|\phi^t_{J\alpha}\rangle\end{aligned} \tag{15}$$

$$\begin{aligned}\langle\Psi_S|H_{SO}|\Psi^{-1}_T\rangle = & \frac{1}{\sqrt{2}}\sum_I\langle\phi^s_{I\alpha}|H_{SO}|\phi^t_{I\beta}\rangle\\ & -\frac{1}{\sqrt{2}}\sum_{I,J}\langle\phi^0_{J\alpha}|H_{SO}|\phi^0_{I\beta}\rangle\langle\phi^s_{I\beta}|\phi^t_{J\beta}\rangle\end{aligned} \tag{16}$$

SOC matrix elements between excited triplets (some combinations of m_s quantum numbers yield zero coupling):

$$\begin{aligned}\langle\Psi^0_{T1}|H_{SO}|\Psi^{+1}_{T2}\rangle = & \frac{1}{\sqrt{2}}\sum_I\langle\phi^{t1}_{I\beta}|H_{SO}|\phi^{t2}_{I\alpha}\rangle\\ & -\frac{1}{\sqrt{2}}\sum_{I,J}\langle\phi^0_{J\beta}|H_{SO}|\phi^0_{I\alpha}\rangle\langle\phi^{t1}_{I\alpha}|\phi^{t2}_{J\alpha}\rangle\end{aligned} \tag{17}$$

$$\begin{aligned}\langle\Psi^0_{T1}|H_{SO}|\Psi^{-1}_{T2}\rangle = &\frac{1}{\sqrt{2}}\sum_I\langle\phi^{t1}_{I\alpha}|H_{SO}|\phi^{t2}_{I\beta}\rangle \\ &-\frac{1}{\sqrt{2}}\sum_{I,J}\langle\phi^0_{J\alpha}|H_{SO}|\phi^0_{I\beta}\rangle\langle\phi^{t1}_{I\beta}|\phi^{t2}_{J\beta}\rangle\end{aligned} \tag{18}$$

$$\begin{aligned}\langle\Psi^{+1}_{T1}|H_{SO}|\Psi^{+1}_{T2}\rangle = &\sum_I\langle\phi^{t1}_{I\alpha}|H_{SO}|\phi^{t2}_{I\alpha}\rangle + \langle\phi^{t1}_{I\alpha}|\phi^{t2}_{I\alpha}\rangle\left[\sum_{i,\sigma}\langle\phi^0_{i\sigma}|H_{SO}|\phi^0_{i\sigma}\rangle\right] \\ &-\sum_{I,J}\langle\phi^0_{J\alpha}|H_{SO}|\phi^0_{I\alpha}\rangle\langle\phi^{t1}_{I\alpha}|\phi^{t2}_{J\alpha}\rangle\end{aligned} \tag{19}$$

$$\begin{aligned}\langle\Psi^{-1}_{T1}|H_{SO}|\Psi^{-1}_{T2}\rangle = &\sum_I\langle\phi^{t1}_{I\beta}|H_{SO}|\phi^{t2}_{I\beta}\rangle + \langle\phi^{t1}_{I\beta}|\phi^{t2}_{I\beta}\rangle\left[\sum_{i,\sigma}\langle\phi^0_{i\sigma}|H_{SO}|\phi^0_{i\sigma}\rangle\right] \\ &-\sum_{I,J}\langle\phi^0_{J\beta}|H_{SO}|\phi^0_{I\beta}\rangle\langle\phi^{t1}_{I\beta}|\phi^{t2}_{J\beta}\rangle\end{aligned} \tag{20}$$

One possible Hamiltonian to include the SOC effects is the ZORA Hamiltonian[9] which is expressed as:

$$H^{ZORA}_{SO} = \frac{c^2}{(2c^2-V)^2}\,\sigma\cdot(\nabla\mathbf{V}\times\mathbf{p}) \tag{21}$$

where c is the speed of light, V formally contains the nuclear field, the electron Coulomb and the xc potentials (although it is usually replaced by van Wüllen's model potential[10]), $\mathbf{p}$ is the three-dimensional momentum operator and σ is the three-dimensional vector of the Pauli matrices.

It has been shown in the above cited paper that the matrix elements of the ZORA SOC with respect to spin-orbitals can be expressed as:

$$\langle\phi_{j\gamma}|H^{ZORA}_{SO}|\phi_{k\delta}\rangle = i\sum_{lmn}\varepsilon_{lmn}\langle\frac{\partial\phi_j}{\partial x_m}|\frac{V}{4c^2-2V}|\frac{\partial\phi_k}{\partial x_n}\rangle\langle\gamma|\sigma_l|\delta\rangle \tag{22}$$

where i is the unit imaginary number and ε_{lmn} is the Levi-Civita tensor.

The CP2K implementation combines the general SOC matrix elements as listed above with the ZORA Hamiltonian.

3 Detailed kernel scaling

Evaluating the RI 3-center integrals $(pq|\mu)$ for the kernel involves a few optimization steps, which themselves come at a cost. First of all, a lot of screening takes place, as not all overlapping basis functions $\varphi_p(\mathbf{r})$, $\varphi_q(\mathbf{r})$ contribute to a particular kernel integral. In particular, for the Hartree and exchange-correlation kernel, the AO integrals are eventually contracted into a mixed AO and MO integrals $(pi_\sigma|\mu)$, where $\phi_{i_\sigma}(\mathbf{r})$ is a core KS orbital. Since the core orbital is local in space, only a few AOs are actually involved. Thus, to save on expensive integral evaluations, a loop over all overlapping $\varphi_p(\mathbf{r})$, $\varphi_q(\mathbf{r})$ is done to check which need to be considered. This is also very present when projecting the density on the RI basis and 3-center overlap integrals $(pq\mu)$ need to be evaluated. In a certain measure, this also happens for the HFX kernel because of the finite range of the exchange potential.

In CP2K's matrix library DBCSR, matrices are split in atomic blocks which are themselves distributed over the processors. The default distribution is optimized for the load balance of the overlap matrix. This is however not the best for the evaluation of our RI integrals which are heavily localized around the current excited atom. Thus, an a newly optimized distribution for the calculation of the $(pq|\mu)$ integrals is determined for each excited atom. However, after evaluation, integrals must be redistributed to match the standard distribution, which comes with an overhead.

Figures 6 and 7 show the detailed timings and scaling of integral evaluations, screening and redistributing for the water and sodium aluminate systems respectively. As expected, the actual integral evaluation scales linearly (measure scalings are 1.0 and 0.8). Due to increasing sparsity, the number of overlap matrix elements increases linearly with system size. However, since screening happens for each excited atom, its overall scaling becomes quadratic (measured at 2.2 and 2.1). Finally, the scaling of integral redistribution was measured at 1.8 and 1.6.

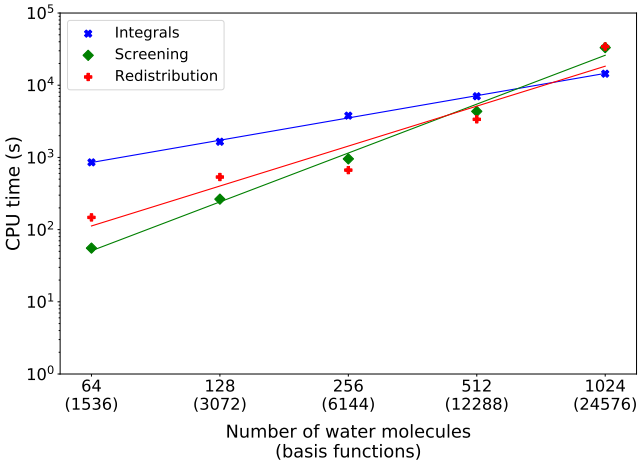

Figure 6 Scaling of the 3-center RI integrals $(pq|\mu)$ evaluations and optimization steps for water cells of increasing sizes. The ADMM-PBEh($\alpha = 0.45$) functional with 6 Å truncation radius and all-electron pcseg-1/admm-1 basis sets are used.

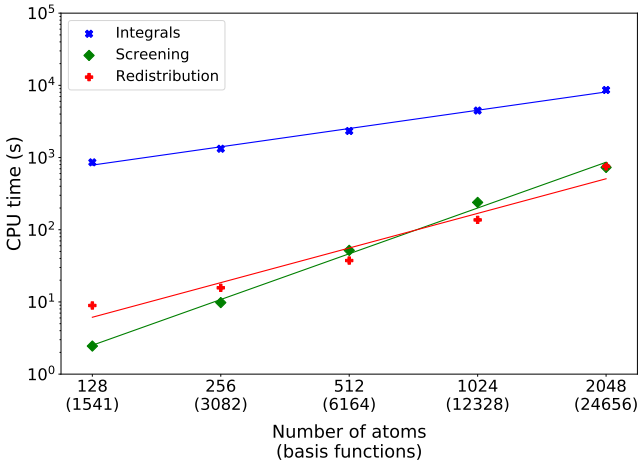

Figure 7 Scaling of the 3-center RI integrals $(pq|\mu)$ evaluations and optimization steps for sodium aluminate cells of increasing sizes. The functional is ADMM-PBEh($\alpha = 0.45$) with 5 Å truncation radius. All-electron pcseg-1/admm-1 basis sets are used for excited aluminium atoms and DZVP-MOLOPT-SR-GTH/FIT3 together with GTH pseudopotentials for the rest.

4 Representative input files

In the following pages, five representative CP2K input files are given. The first two files, in sections 4.1 and 4.2, were used for K-edge and L-edge validation, respectively. Because these are benchmark calculations, numerical accuracy is primordial. This is ensured by very high plane wave cutoffs, dense grids and minimal integral screening. The L-edge calculation has spin–orbit coupling enabled and therefore requires both singlet and triplet calculations (default is singlet only).

The input file in section 4.3 is representative for the ADMM acceleration benchmark study. It is essentially the same as the first two, with the addition of of the &AUXILIARY_DENSITY_MATRIX_METHOD section and AUX_FIT auxiliary basis sets.

The last two input files, in sections 4.4 and 4.5, are representative of periodic boundary calculations such as those for extended system and scaling studies, respectively. They are characterized by lower plane wave cutoffs, less dense grids and increase integral screening. Note that because of the PBCs, the truncated Coulomb potential is used.

4.1 K-edge validation

CO molecule, carbon and oxygen K-edge, B3LYP/cc-pCVTZ input file:

```
&GLOBAL
  PROJECT CO
  PRINT_LEVEL LOW
  RUN_TYPE ENERGY
&END GLOBAL
&FORCE_EVAL
  METHOD Quickstep
  &DFT
    BASIS_SET_FILE_NAME BASIS_XAS_PAPER
    POTENTIAL_FILE_NAME POTENTIAL
    AUTO_BASIS RI_XAS LARGE

    &MGRID
      CUTOFF 1600
      REL_CUTOFF 50
      NGRIDS 5
    &END MGRID

    &QS
      METHOD GAPW
    &END QS
    &POISSON
      PERIODIC NONE
      PSOLVER MT
    &END
    &SCF
      EPS_SCF 1.0E-8
      MAX_SCF 25
      &OT
        MINIMIZER DIIS
        PRECONDITIONER FULL_ALL
        ENERGY_GAP 0.001
      &END OT
      &OUTER_SCF
        MAX_SCF 4
        EPS_SCF 1.0E-8
      &END OUTER_SCF
    &END SCF

    &XC
      &XC_FUNCTIONAL
        &LIBXC
          FUNCTIONAL HYB_GGA_XC_B3LYP
        &END LIBXC
      &END XC_FUNCTIONAL
      &HF
        FRACTION 0.2
        &SCREENING
          EPS_SCHWARZ 1.0E-16
        &END SCREENING
      &END HF
    &END XC
    . . .
    . . .
    &XAS_TDP
      &DONOR_STATES
        DEFINE_EXCITED BY_KIND
        KIND_LIST C O
        STATE_TYPES 1s 1s
        N_SEARCH 2
      &END DONOR_STATES

      GRID C 974 3000
      GRID O 974 3000

      DIPOLE_FORM LENGTH
      TAMM_DANCOFF FALSE
      N_EXCITED 12

      &KERNEL
        RI_REGION 5.0
        &XC_FUNCTIONAL
          &LIBXC
            FUNCTIONAL HYB_GGA_XC_B3LYP
          &END LIBXC
        &END XC_FUNCTIONAL
        &EXACT_EXCHANGE
          FRACTION 0.2
          EPS_SCREEN 1.0E-16
        &END EXACT_EXCHANGE
      &END KERNEL
    &END XAS_TDP
  &END DFT

  &SUBSYS
    &CELL
      ABC 10.0 10.0 10.0
      PERIODIC NONE
    &END CELL
    &TOPOLOGY
      COORD_FILE_FORMAT XYZ
      COORD_FILE_NAME CO.xyz
      &CENTER_COORDINATES
      &END CENTER_COORDINATES
    &END TOPOLOGY
    &KIND C
      BASIS_SET cc-pCVTZ
      POTENTIAL ALL
      RADIAL_GRID 80
      LEBEDEV_GRID 120
    &END KIND
    &KIND O
      BASIS_SET cc-pCVTZ
      POTENTIAL ALL
      RADIAL_GRID 80
      LEBEDEV_GRID 120
    &END KIND
  &END SUBSYS
&END FORCE_EVAL
```

4.2 L-edge validation

$SiCl_4$ molecule, silicon L-edge with SOC, B3LYP/def2-TZVPD input file:

```
&GLOBAL
 PROJECT SiCl4
 PRINT_LEVEL LOW
 RUN_TYPE ENERGY
&END GLOBAL
&FORCE_EVAL
 &DFT
  BASIS_SET_FILE_NAME BASIS_XAS_PAPER
  POTENTIAL_FILE_NAME POTENTIAL
  AUTO_BASIS RI_XAS LARGE

  &POISSON
   PERIODIC NONE
   PSOLVER MT
  &END POISSON
  &QS
   METHOD GAPW
  &END QS

  &MGRID
   CUTOFF 1600
   REL_CUTOFF 50
   NGRIDS 5
  &END

  &SCF
   EPS_SCF 1.0E-8
   MAX_SCF 200
   &MIXING
     METHOD BROYDEN_MIXING
     ALPHA 0.2
     BETA 1.5
     NBROYDEN 8
   &END MIXING
  &END SCF

  &XC
   &XC_FUNCTIONAL
     &LIBXC
       FUNCTIONAL HYB_GGA_XC_B3LYP
     &END LIBXC
   &END XC_FUNCTIONAL
   &HF
     FRACTION 0.2
     &SCREENING
       EPS_SCHWARZ 1.0E-16
     &END SCREENING
   &END HF
  &END XC
  ...
  ...
  &XAS_TDP
   &DONOR_STATES
     DEFINE_EXCITED BY_KIND
     KIND_LIST Si
     STATE_TYPES 2p
   &END DONOR_STATES

   TAMM_DANCOFF FALSE
   DIPOLE_FORM LENGTH

   GRID Si 974 3000

   EXCITATIONS RCS_SINGLET
   EXCITATIONS RCS_TRIPLET
   SOC

   &KERNEL
     RI_REGION 5.0
     &XC_FUNCTIONAL
       &LIBXC
         FUNCTIONAL HYB_GGA_XC_B3LYP
       &END LIBXC
     &END XC_FUNCTIONAL
     &EXACT_EXCHANGE
       FRACTION 0.2
       EPS_SCREEN 1.0E-16
     &END EXACT_EXCHANGE
   &END KERNEL
  &END XAS_TDP
&END DFT

&SUBSYS
 &KIND Si
   BASIS_SET def2-TZVPD
   POTENTIAL ALL
   RADIAL_GRID 100
   LEBEDEV_GRID 150
 &END KIND
 &KIND Cl
   BASIS_SET def2-TZVPD
   POTENTIAL ALL
   RADIAL_GRID 100
   LEBEDEV_GRID 150
 &END KIND
 &CELL
   ABC 10.0 10.0 10.0
   PERIODIC NONE
 &END CELL
 &TOPOLOGY
   COORD_FILE_FORMAT XYZ
   COORD_FILE_NAME SiCl4.xyz
   &CENTER_COORDINATES
   &END CENTER_COORDINATES
 &END TOPOLOGY
&END SUBSYS  &END FORCE_EVAL
```

4.3 ADMM acceleration

Water molecule (CAS number: 7732-18-5), oxygen K-edge, ADMM—B3LYP/pcseg-1—admm-1 input file:

```
&GLOBAL
 PROJECT 7732-18-5
 PRINT_LEVEL LOW
 RUN_TYPE ENERGY
&END GLOBAL
&FORCE_EVAL
 METHOD Quickstep
 &DFT
  BASIS_SET_FILE_NAME BASIS_XAS_PAPER
  POTENTIAL_FILE_NAME POTENTIAL
  AUTO_BASIS RI_XAS MEDIUM

  &AUXILIARY_DENSITY_MATRIX_METHOD
    ADMM_PURIFICATION_METHOD NONE
  &END AUXILIARY_DENSITY_MATRIX_METHOD

  &MGRID
    CUTOFF 1000
    REL_CUTOFF 50
    NGRIDS 5
  &END MGRID

  &QS
    METHOD GAPW
  &END QS
  &POISSON
    PERIODIC NONE
    PSOLVER MT
  &END
  &SCF
    EPS_SCF 1.0E-8
    MAX_SCF 500

    &MIXING
      METHOD BROYDEN_MIXING
      ALPHA 0.2
      BETA 1.5
      NBROYDEN 8
    &END MIXING
  &END SCF

  &XC
    &XC_FUNCTIONAL
      &LIBXC
        FUNCTIONAL HYB_GGA_XC_B3LYP
      &END LIBXC
    &END XC_FUNCTIONAL
    &HF
      FRACTION 0.2
    &END HF
  &END XC
  ...
  ...
  &XAS_TDP
    &DONOR_STATES
      DEFINE_EXCITED BY_KIND
      KIND_LIST O
      STATE_TYPES 1s
      N_SEARCH 1
    &END DONOR_STATES

    GRID O 974 1500

    DIPOLE_FORM LENGTH
    TAMM_DANCOFF TRUE
    N_EXCITED 12

    &KERNEL
      RI_REGION 5.0
      &XC_FUNCTIONAL
        &LIBXC
          FUNCTIONAL HYB_GGA_XC_B3LYP
        &END LIBXC
      &END XC_FUNCTIONAL
      &EXACT_EXCHANGE
        FRACTION 0.2
      &END EXACT_EXCHANGE
    &END KERNEL
  &END XAS_TDP
 &END DFT
 &SUBSYS
  &CELL
    ABC 10.0 10.0 10.0
    PERIODIC NONE
  &END CELL
  &TOPOLOGY
    COORD_FILE_FORMAT XYZ
    COORD_FILE_NAME 7732-18-5.xyz
    &CENTER_COORDINATES
    &END CENTER_COORDINATES
  &END TOPOLOGY
  &END KIND
  &KIND O
    BASIS_SET pcseg-1
    BASIS_SET AUX_FIT admm-1
    POTENTIAL ALL
    RADIAL_GRID 100
    LEBEDEV_GRID 160
  &END KIND
  &KIND H
    BASIS_SET pcseg-1
    BASIS_SET AUX_FIT admm-1
    POTENTIAL ALL
    RADIAL_GRID 100
    LEBEDEV_GRID 160
  &END KIND
 &END SUBSYS
&END FORCE_EVAL
```

4.4 Extended systems

Sodium aluminate crystal in periodic boundary conditions, Al K-edge, ADMM—PBEh($\alpha = 0.45$)/mixed basis sets input file:

```
&GLOBAL
  PROJECT sodal
  RUN_TYPE ENERGY
  PRINT_LEVEL LOW
&END GLOBAL

&FORCE_EVAL
  METHOD QS
  &DFT
    BASIS_SET_FILE_NAME BASIS_ADMM
    BASIS_SET_FILE_NAME BASIS_XAS_PAPER
    BASIS_SET_FILE_NAME BASIS_MOLOPT
    POTENTIAL_FILE_NAME POTENTIAL
    AUTO_BASIS RI_XAS MEDIUM

    &QS
      METHOD GAPW
    &END QS

    &AUXILIARY_DENSITY_MATRIX_METHOD
      ADMM_PURIFICATION_METHOD NONE
    &END AUXILIARY_DENSITY_MATRIX_METHOD

    &SCF
      MAX_SCF 30
      EPS_SCF 1.0E-06
      SCF_GUESS ATOMIC

      &OT
       MINIMIZER DIIS
       PRECONDITIONER FULL_ALL
      &END OT
      &OUTER_SCF
        MAX_SCF 6
        EPS_SCF 1.0E-06
      &END
    &END SCF

    &MGRID
      CUTOFF 400
      REL_CUTOFF 40
      NGRIDS 5
    &END

    &XC
      &XC_FUNCTIONAL PBE
        &PBE
          SCALE_X 0.55
        &END
      &END XC_FUNCTIONAL

      &HF
        FRACTION 0.45
        &INTERACTION_POTENTIAL
          POTENTIAL_TYPE TRUNCATED
          CUTOFF_RADIUS 5.0
        &END INTERACTION_POTENTIAL
        &SCREENING
          EPS_SCHWARZ 1.0E-6
        &END SCREENING
      &END HF
    &END XC
    ...
    ...
    &XAS_TDP
      &DONOR_STATES
        DEFINE_EXCITED BY_KIND
        KIND_LIST Alx
        STATE_TYPES 1s
        N_SEARCH 1
      &END DONOR_STATES

      TAMM_DANCOFF
      GRID Alx 150 300
      ENERGY_RANGE 20.0

      &OT_SOLVER
        MINIMIZER DIIS
        EPS_ITER 1.0E-4
      &END OT_SOLVER

      &KERNEL
        &XC_FUNCTIONAL PBE
          &PBE
            SCALE_X 0.55
          &END
        &END XC_FUNCTIONAL
        &EXACT_EXCHANGE
          OPERATOR TRUNCATED
          RANGE 5.0
          SCALE 0.45
        &END EXACT_EXCHANGE
      &END KERNEL
    &END XAS_TDP
  &END DFT

  &SUBSYS
    &CELL
      ABC 10.467947 10.651128 14.393541
    &END CELL
    &TOPOLOGY
      COORD_FILE_NAME geopt.xyz
      COORD_FILE_FORMAT xyz
    &END TOPOLOGY
   &KIND O
    BASIS_SET DZVP-MOLOPT-SR-GTH
    BASIS_SET AUX_FIT FIT3
    POTENTIAL GTH-PBE
   &END KIND
   &KIND Na
    ELEMENT Na
    BASIS_SET DZVP-MOLOPT-SR-GTH
    BASIS_SET AUX_FIT FIT3
    POTENTIAL GTH-PBE
   &END
   &KIND Al
    BASIS_SET DZVP-MOLOPT-SR-GTH
    BASIS_SET AUX_FIT FIT3
    POTENTIAL GTH-PBE
   &END
   &KIND Alx
    ELEMENT Al
    BASIS_SET pcseg-2
    BASIS_SET AUX_FIT admm-2
    POTENTIAL ALL
   &END
  &END SUBSYS
&END FORCE_EVAL
```

4.5 Scaling

Periodic box of 1024 water molecules, oxygen K-edge, ADMM—PBEh($\alpha = 0.45$)/pcseg-1—admm-1 input file:

```
&GLOBAL
  PROJECT 1024
  RUN_TYPE ENERGY
  PRINT_LEVEL MEDIUM
  &TIMINGS
     THRESHOLD 0.0001
  &END TIMINGS
&END GLOBAL
&FORCE_EVAL
  METHOD QS
  &DFT
    BASIS_SET_FILE_NAME BASIS_XAS_PAPER
    POTENTIAL_FILE_NAME POTENTIAL
    AUTO_BASIS RI_XAS SMALL

    WFN_RESTART_FILE_NAME 1024-RESTART.wfn

    &QS
      METHOD GAPW
    &END QS

    &MGRID
      CUTOFF 400
      REL_CUTOFF 40
      NGRIDS 5
    &END MGRID

    &SCF
      SCF_GUESS RESTART
      EPS_SCF 1.0E-6
      MAX_SCF 30

      &OT
        MINIMIZER DIIS
        PRECONDITIONER FULL_ALL
      &END OT

      &OUTER_SCF
        MAX_SCF 6
        EPS_SCF 1.0E-6
      &END OUTER_SCF
    &END SCF

    &AUXILIARY_DENSITY_MATRIX_METHOD
      ADMM_PURIFICATION_METHOD NONE
    &END AUXILIARY_DENSITY_MATRIX_METHOD

    &XC
      &HF
        FRACTION 0.45
        &INTERACTION_POTENTIAL
          POTENTIAL_TYPE TRUNCATED
          CUTOFF_RADIUS 6.0
        &END INTERACTION_POTENTIAL
        &SCREENING
          EPS_SCHWARZ 1.0E-6
        &END SCREENING
        &MEMORY
          MAX_MEMORY 0
        &END MEMORY
      &END HF
      ...
      ...
      &XC_FUNCTIONAL PBE
        &PBE
          SCALE_X 0.55
        &END PBE
      &END XC_FUNCTIONAL
    &END XC

    &XAS_TDP
      &DONOR_STATES
        DEFINE_EXCITED BY_KIND
        KIND_LIST O
        STATE_TYPES 1s
        N_SEARCH 1024
        LOCALIZE
      &END DONOR_STATES

      TAMM_DANCOFF
      GRID O 120 200
      E_RANGE 16.0

      &OT_SOLVER
        MINIMIZER DIIS
        EPS_ITER 1.0E-4
      &END OT_SOLVER

      &KERNEL
        &XC_FUNCTIONAL PBE
          &PBE
            SCALE_X 0.55
          &END PBE
        &END XC_FUNCTIONAL
        &EXACT_EXCHANGE
          OPERATOR TRUNCATED
          CUTOFF_RADIUS 6.0
          FRACTION 0.45
        &END EXACT_EXCHANGE
      &END KERNEL

    &END XAS_TDP
  &END DFT
  &SUBSYS
    &CELL
      ABC 31.3250 31.3250 31.3250
    &END CELL
    &TOPOLOGY
      COORD_FILE_FORMAT XYZ
      COORD_FILE_NAME 1024.xyz
    &END TOPOLOGY
    &KIND H
      BASIS_SET pcseg-1
      BASIS_SET AUX_FIT admm-1
      POTENTIAL ALL
    &END KIND
    &KIND O
      BASIS_SET pcseg-1
      BASIS_SET AUX_FIT admm-1
      POTENTIAL ALL
    &END KIND
  &END SUBSYS
&END FORCE_EVAL
```

Notes and references

[1] M. L. Vidal, X. Feng, E. Epifanovsky, A. I. Krylov and S. Coriani, *Journal of Chemical Theory and Computation*, 2019, **15**, 3117–3133.

[2] J. Schirmer, A. Trofimov, K. Randall, J. Feldhaus, A. Bradshaw, Y. Ma, C. Chen and F. Sette, *Physical Review A*, 1993, **47**, 1136.

[3] M. Domke, C. Xue, A. Puschmann, T. Mandel, E. Hudson, D. Shirley and G. Kaindl, *Chemical Physics Letters*, 1990, **173**, 122–128.

[4] M. Tronc, G. C. King and F. Read, *Journal of Physics B: Atomic and Molecular Physics*, 1979, **12**, 137.

[5] R. Püttner, I. Dominguez, T. Morgan, C. Cisneros, R. Fink, E. Rotenberg, T. Warwick, M. Domke, G. Kaindl and A. Schlachter, *Physical Review A*, 1999, **59**, 3415.

[6] F. Franco de Carvalho, B. F. Curchod, T. J. Penfold and I. Tavernelli, *The Journal of Chemical Physics*, 2014, **140**, 144103.

[7] R. Bauernschmitt and R. Ahlrichs, *Chemical Physics Letters*, 1996, **256**, 454–464.

[8] P.-O. Löwdin, *Physical Review*, 1955, **97**, 1474.

[9] E. van Lenthe, J. G. Snijders and E. J. Baerends, *The Journal of Chemical Physics*, 1996, **105**, 6505–6516.

[10] C. van Wüllen, *The Journal of Chemical Physics*, 1998, **109**, 392–399.